Purdue University
Purdue e-Pubs

Birck and NCN Publications | Birck Nanotechnology Center

5-27-2009

Quantum Confined Stark Shift and Ground State Optical Transition Rat in [100] Laterally Biased InAs/GaAs Quantum Dots

Muhammad Usman
Purdue University - Main Campus

Hoon Ryu
Purdue University - Main Campus

Sunhee Lee
Purdue University - Main Campus

Yui H. Tan
Purdue University - Main Campus

Gerhard Klimeck
Purdue University - Main Campus, gekco@purdue.edu

Follow this and additional works at: https://docs.lib.purdue.edu/nanopub

Usman, Muhammad; Ryu, Hoon; Lee, Sunhee; Tan, Yui H.; and Klimeck, Gerhard, "Quantum Confined Stark Shift and Ground State Optical Transition Rat in [100] Laterally Biased InAs/GaAs Quantum Dots" (2009). *Birck and NCN Publications.* Paper 425.
https://docs.lib.purdue.edu/nanopub/425

This document has been made available through Purdue e-Pubs, a service of the Purdue University Libraries. Please contact epubs@purdue.edu for additional information.

Quantum Confined Stark Shift and Ground State Optical Transition Rate in [100] Laterally Biased InAs/GaAs Quantum Dots

Muhammad Usman[1*], Hoon Ryu[1*], Sunhee Lee[1], Yui H. Tan[1], and Gerhard Klimeck[1,2]

[1] *Network for Computational Nanotechnology, Electrical and Computer Engineering, Purdue University, W. Lafayette, IN 47907, USA*
[2]*Jet Propulsion Laboratory, California Institute of Technology, Pasadena, CA 91109*
Email: {usman, ryu2}@purdue.edu
[*]*Authors contributed equally*

***Abstract* – The atomistic tight binding simulator NEMO 3-D has previously been validated against the experimental data for quantum dots, wells, and wires in the InGaAlAs and SiGe material systems. Here, we demonstrate our new capability to compute optical matrix elements and transition strengths in tight binding. Systematic multi-million atom electronic structure calculations explore the quantum confined stark shift and the ground state optical transition rate for an electric field in the lateral [100] direction. The simulations treat the strain in a ~15 million atom system and the electronic structure in a subset of ~9 million atoms. The effects of the long range strain, the optical polarization anisotropy, the interface roughness, and the non-degeneracy of the p-states which are missing in continuum methods like effective mass approximation or k•p are included. A significant red shift in the emission spectra due to an applied in-plane electric field indicating a strong quantum confined stark effect (QSCE) is observed. The ground state optical transition rate rapidly decreases with the increasing electric field magnitude due to reduced spatial overlap of ground electron and hole states.**

Keywords - Stark effect, Strain, Quantum Dot, lateral field, transition rate.

I – INTRODUCTION

Self-assembled InAs-GaAs quantum dots [1, 2] have been extensively studied for their potential applications in the quantum dot lasers [3], optical communication devices at long wavelength [4-8], photo-detectors [9], and as quantum gates for quantum computing applications [10]. While the asymmetric quantum confined stark effect (QCSE) and the presence of a permanent dipole moment due to a vertically applied electric field are well known and have been studied in detail in the past [11-14], very little is known about the dependence of the ground state transition energy, the optical transition rate and the carrier wave function response to an applied in-plane electric field. In contrast to the vertical field results, experiments [15, 16] have demonstrated the absence of an in-plane dipole moment in the lateral direction. No theoretical study of this experimental evidence is present in the literature to date. This paper provides a theoretical study to qualitatively and quantitatively analyze the behavior of the quantum dot structures for an applied [100] electrical field.

A full band atomistic tight binding model is applied to study the ground state optical transition rate. The inter-band optical transition rate is calculated using the Fermi's Golden [17] which has been well-known in the quantum physics. However, its application to multi-million atom systems has not been shown in the literature to date. Although a couple of previous studies [18, 19] have computed optical matrix elements with the effective mass or k•p approximation, such continuum methods are limited in missing the optical polarization anisotropy, the interface roughness, and the non-degeneracy of the p-states. Here we show that a small (possible experimentally hard to measure) lateral dipole moment exists. We also show that electric field decreases the spatial overlap between electron and hole wave functions significantly, resulting in a rapid decrease in the optical transition rate.

II – METHODOLOGY

NEMO 3-D can atomistically simulate realistic systems as large as containing up to 52 million atoms [20]. The electronic structure is calculated using a twenty band $sp^3d^5s^*$ nearest neighbor empirical tight binding model [21] and the strain with an atomistic valence force field (VFF) method [22]. The $sp^3d^5s^*$ tight binding parameters are fit to reproduce the bulk properties of GaAs, InAs, AlAs, Si, and Ge with respect to room temperature band edges, effective masses, hydrostatic/bi-axial strain behavior, and relative band edges [24] using a global minimization procedure based on a genetic algorithm [25]. Rather than using an averaged potential representation, the strain and electronic structure properties of alloys and interfaces are reproduced through an explicit disordered atomistic representation [24]. For realistic nano-scale systems, our $sp^3d^5s^*$ tight binding approach employed in NEMO 1-D, and NEMO 3-D, has been validated experimentally through 1) high bias, high current, quantitative resonant tunneling diode modeling [26], 2) photoluminescence in InAs nanoparticles [27], 3) modeling of the Stark effect of single P impurities in Si [28], 4) distinguishing P and As impurities in ultra-scaled FinFET devices [29] 5) the valley splitting in miscut Si quantum wells on SiGe substrate [30] and 6) InAs/InGaAs/GaAs quantum dot designs without any material parameter adjustments [31].

From Fermi's golden rule, the optical matrix element T is computed from Eq. 1, where the momentum matrix M is given in equation 2 [32]:

$$T = |< \Phi_c \mid M \mid \Phi_v >|^2 \qquad (1)$$

$$M = \frac{m_0}{i\hbar}[\vec{n}, H] \qquad (2)$$

where, $\Phi_{c/v}$ are the wave functions describing the ground electron and hole state, respectively, H is the single particle

978-1-4244-3927-0/09/$25.00 ©2009 IEEE

Authorized licensed use limited to: Purdue University. Downloaded on October 19, 2009 at 15:42 from IEEE Xplore. Restrictions apply.

Hamiltonian and the light is assumed to cause a polarization along the direction n and m_0 is the free electron mass.

Previous studies use the charge overlap [33, 34] to estimate the optical transition rate (Eq. 3) that does not include the polarization of the induced light. In this study, we have used the first moment of spatial overlap in x direction (Eq. 4) to take into account the polarization of the incident light. In section five, we compare the results of two methods for the [100] applied bias:

$$<|\Phi_c|^2||\Phi_v|^2> \quad (3)$$

$$|<\Phi_c|\vec{n}|\Phi_v>|^2 \quad (4)$$

III – SIMULATED SYSTEM

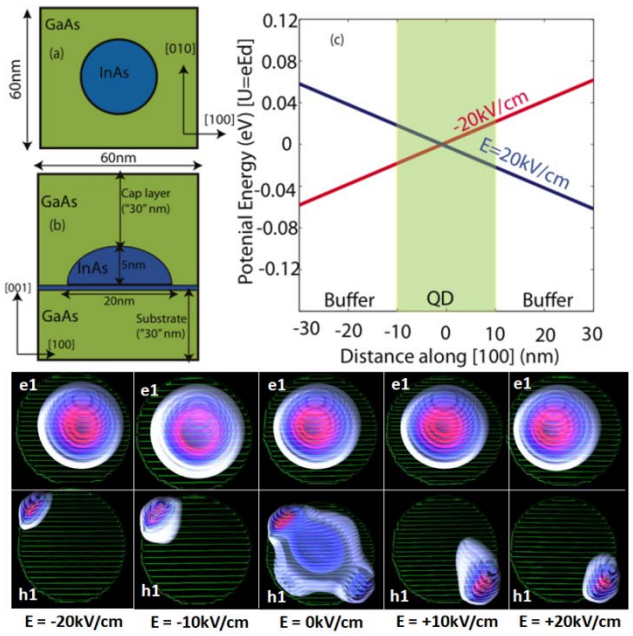

Figure 1: (a, b) Schematic views of the system simulated in [100, 001] and [100, 010] planes. A dome shaped InAs quantum dot with diameter 20nm and height 5nm is placed on a 0.5 nm InAs wetting layer. A 60x60x66nm GaAs buffer surrounds the quantum dot. (c) Potential energy profile in the [100] direction as a function of the distance for the applied [100] electric fields of values 20kV/cm and -20kV/cm. Bottom two rows show the Top view of the ground state hole (h_1) wave function and electron (e_1) wave functions for the applied electric field E_x of 0kV/cm, -10kV/cm, -10kV/cm, +20kV/cm, and -20kV/cm. Only the quantum dot and surrounding region is shown for clarity. Green color shows the quantum dot boundary. Blue and red color show the intensity of the magnitude (red is highest and blue is lowest)

Figure 1(a, b) shows the schematic of the system simulated which consists of a dome shaped InAs quantum dot (QD) of 5nm height and 20nm base diameter on a 1ML InAs wetting layer. A large GaAs buffer (a total volume of 60x60x66 nm^3) containing 15.6 million atoms surrounds the whole structure which is used for the atomistic strain calculation. The strain simulations fix the atom positions on the bottom plane to the GaAs lattice constant, assume periodic boundary conditions in the lateral dimensions, and open boundary condition on the top surface. Physical intuition tells us that the states of interest are confined in the region around the QD. Numerical experiments validate that the electronic structure computation can be performed in a smaller region (50nm in the lateral dimension and 56nm in the growth direction consisting of 8.96 million atoms) around the InAs QD without the loss of accuracy, after the atom positions have been computed in the large domain, therefore including the long-range strain interaction. The smaller electronic box assumes closed boundary conditions with passivated dangling bonds [35]. These multi-million atomic simulations run on ~80 CPU's for about 15-20 hours. A constant electric field E_x varying from -20kV/cm to +20kV/cm is applied in the [100] direction. Figure 1(c) shows the potential energy ($U_e = e.E_x.d$, where e is the electron charge, E_x is the applied electrical field and d is the distance along [100] direction) profile along [100] direction through the center of the quantum dot [y=30nm, z=31nm].

The last two rows of the figure 1 show the ground hole (h_1) and electron (e_1) wave functions. The ground electron wave function have a very symmetric round shape while the hole wave function is aligned along [1$\underline{1}$0] direction. This alignment of hole wave function can be attributed to the long range strain effects that breaks the crystal symmetry and favors the [110] and [1$\underline{1}$0] directions. Similar explanation for [110] and [1$\underline{1}$0] aligned excited electron states can be found in the literature [36, 37]. The alignment of the hole wave functions along [1$\underline{1}$0] direction will result in the stronger dipole moment and larger optical transition rate in this direction as compared to the [100] direction. We are currently studying this effect and the results will be published elsewhere.

Figure 1 shows that the application of the external electrical field shifts the hole and electron wave functions in the opposite direction significantly. The hole wave function is moved much more significantly and can be seen concentrated on the boundary of the quantum dot for non-zero electric field magnitude. This significantly reduces the overlap between the wave functions, thus causing rapid decrease in the optical transition rate described in section IV.

IV – QUANTUM CONFINED STARK EFFECT

Figure 2 (a, b) shows the plot of ground electron and hole energy levels respectively as a function of the applied in-plane electric field E_x. Figure 3 plots the ground state transition energy (the optical gap) of the system ($e_T = e_1 - h_1$) as a function of the applied in-plane electric field. A significant amount of red shift is observed for the applied electric field due to the quantum confined stark effect (QCSE). A parabolic red shift of 10.3meV for 20kV/cm applied electric field is observed.

The dependence of the transition energy e_T on the applied electric field is defined by a quadratic relation in the literature [11-16],

$$e_T(E) = e_T(0) + \rho E + \beta E^2 \quad (5)$$

where $e_T(0)$ and $e_T(E)$ are the ground state transition energies with the applied electric field values of zero and E, respectively. ρ depends on the built in dipole moment and β is a measure of the polarizibility of the electron and hole wave

Authorized licensed use limited to: Purdue University. Downloaded on October 19, 2009 at 15:42 from IEEE Xplore. Restrictions apply.

functions. This is evident from the figure 3 that the very symmetric dependence of the transition energy on the electric field with respect to |E| = 0kV/cm results in only a small dipole moment in the plane of the quantum dot [12, 13] along the [100] direction. The maximum value of e_T occurs at E_0=+1.4kV/cm. This value may be too small to detect in real systems with other non-idealities. From a least square fit to the equation (5), we find a value of -1.8x10^{-16} (cm.eV/kV) for dipole moment ρ and a value of 13.96 μeV/(kV/cm)^2 for polarizibility β. The polarizibility has a negligibly small dependence on the direction of the applied electrical field in the [100] direction, highlighting a large degree of [100] isotropy for the quantum dots. Such high symmetry conditions are very desirable in view of the generation of entangled photon pairs [16]. The fact that the in-plane dipole moment is very small reduces equation (1) to:

$$e_T(E) = e_T(0) + \beta^* (E-E_0)^2 \qquad (6)$$

From a least square fit to the equation (6) for the calculated data, we find that the polarizibility β^* has a value of about -14 μeV/(kV/cm)^2 which is very close to the value of β found from equation 5 earlier, again implying that the [100] dipole moment is very weak. Our calculated value is close to the experimentally found values of -4 μeV/(kV/cm)^2 in Ref. 15, and -2 to -5 μeV/(kV/cm)^2 in Ref. 16.

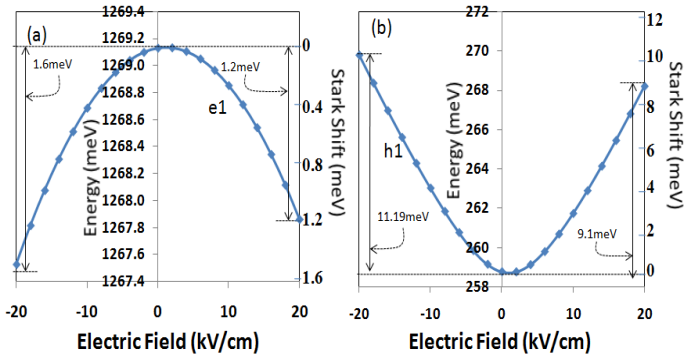

Figure 2: (a) Ground electron and (b) hole energy level as a function of the in-plane electric field E_x.

V – OPTICAL TRANSITION RATE

Figure 4 plots the normalized ground state optical transition rate in the *x* direction as a function of the applied electric field computed in three methods of Eq. 1-4.. The ground state transition rate is calculated as the modulus squared of the optical matrix element for the ground hole and electron state transition summed over the degenerate spin states. The quantum dot under consideration is very flat with a low aspect ratio (height/base = 0.25). For such quantum dots, the ground state matrix element is much larger for the light polarized in the *x*-*y* plane than it is for the light polarized along the growth direction *z* [18]. We find that the transition rate in the *z* direction is about two orders of magnitude smaller than the transition rate along *x*-*y* direction, thus verifying the already published evidence [18].

For the *x* polarized light, we find that as the magnitude of the applied electric field increases, the optical transition rate decreases rapidly. The reduction in the optical transition rate is directly related to the reduced spatial overlap between the electron and hole ground states [18]. Figure 1 (last two rows) plots the ground hole (h_1) and electron (e_1) wave functions for the applied electric fields E_x of 0kV/cm, +10kV/cm, -10kV/cm, +20kV/cm, and -20kV/cm. As the magnitude of the electric field increases, the electron and hole wave functions move in the opposite direction decreasing their spatial overlap.

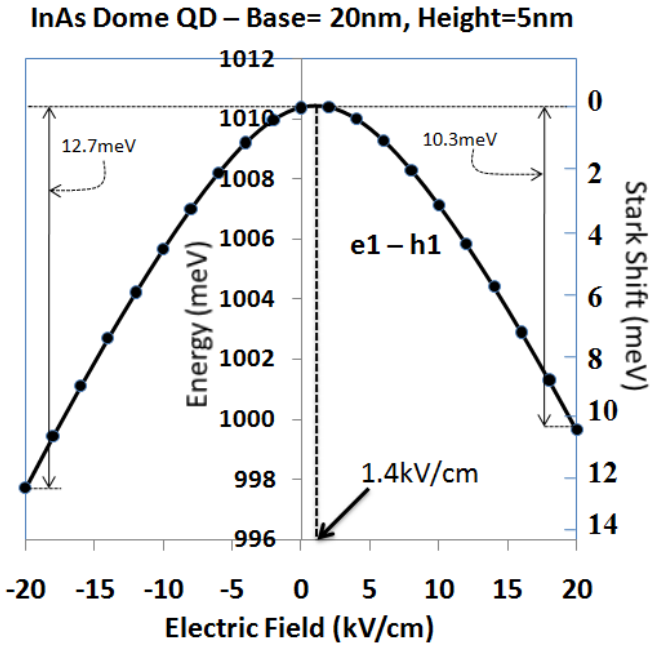

Figure 3: The ground state transition energy (e_T = e_1-h_1) is plotted as a function of the applied electrical field E_x. Scale on the right shows the stark shift in meV. The transition energy dependence on the electric field is highly symmetric with respect to |E| = 0kV/cm indicating a very weak dipole moment "ρ".

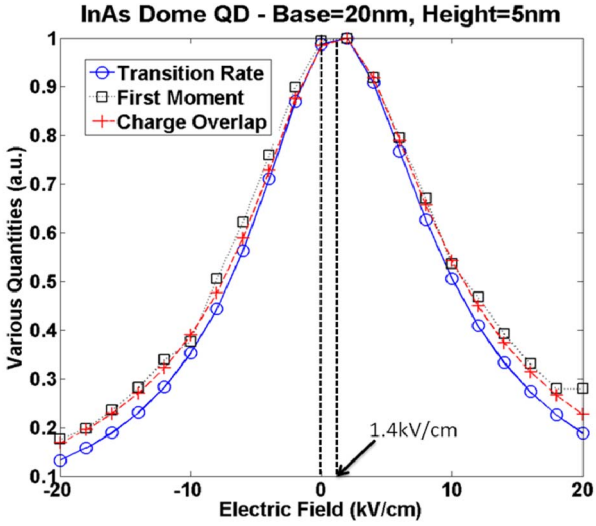

Figure 4: The normalized values of the ground state optical transition rate, first moment of the spatial overlap in the *x* direction, and the charge overlap are shown as a function of the applied electric field. The transition rate rapidly decreases as the applied field magnitude increases. First moment and charge overlap methods give good estimation of the transition rate.

Authorized licensed use limited to: Purdue University. Downloaded on October 19, 2009 at 15:42 from IEEE Xplore. Restrictions apply.

We have used two methods to estimate the decrease in the transition rate described by equations 3 and 4. Figure 4 also plots the normalized values of the charge overlap (Eq. 3) and the first moment in the *x* direction (Eq. 4). Although we believed that the first moment method will give the better estimation of the transition rate because it considers the direction of the polarization of the incident light, both methods show similar results for this particular study. This is because the spatial overlap of the wave functions does not have significant *x* dependence. We are currently exploring these two methods for different quantum dot heights and base diameters. In our future work, we will show a detailed comparison of these two methods for various quantum dot geometries.

In conclusion, our atomistic tight binding simulator NEMO 3-D is used to present a study of the in-plane electrical field dependence of the ground state transition energy and the interband optical transition rate in an InAs/GaAs QD system. A quantum confined stark effect (QSCE) of ~3.2meV for the ground state electron-hole transition is observed when the electrical field magnitude increases from 0 to 10kV/cm. Our calculations show a very weak build-in dipole which may be too small to observe experimentally. Finally, we find that the optical transition rate drastically decreases as the electrical field is increased.

This work serves as a validation of our new optical matrix calculation method. We used first moment of spatial overlap and charge overlap methods to calibrate our new, more complete optical transition rate calculation method. In this study, all methods give similar results. A detailed study of these methods for various quantum dot geometries is being done.

The anisotropy of the ground hole wave function will result in the stronger dipole moment and larger optical transition rates. This has not been explored in previous studies and we are in the process of studying this interesting problem in detail. The results will be published elsewhere.

ACKNOWLEDGEMENT

Authors are grateful to Prof. T.B. Boykin (University of Alabama, Huntsville, AL) for useful discussions about the calculation of the transition rate. This work has been carried out in part at the Jet Propulsion Laboratory, California Institute of Technology, under a contract with the National Aeronautics and Space Administrator. Computational resources on nanoHUB.org funded by the National Science Foundation have been extensively used in this work. Muhammad Usman is funded through Fulbright USAID (Grant ID # 15054783).

REFERENCES

[1] L. Jacak, P. Hawrylak, and A. Wojs, Quantum Dots (Springer Berlin, NY, 1998)
[2] D. Bimberg, M. Grundmann, and N. N. Ledentsov, Quantum Dot Heterostructure (John Wiley and Sons Chichester, UK, 1998)
[3] D. L. Huffaker, G. Park, Z. Zou, O.B. Shchekin, and D.G. Deppe, Appl. Phys. Lett. 73, 2564 (1998)
[4] J.Tatebayashi, M. Nishioka, and Y. Arakawa, Appl. Phys. Lett. 78, 3469 (2001).
[5] V. M. Ustinov, N. A. Maleev, A. E. Zhukov, A.R. Kovsh, A. Yu. Egorov, A. V. Lunev, B. V. Volovik, I.L. Krestnikov, Yu. G. Musikhin, N. A. Bert, P.S. Kop'ev, Zh. I. Alfero, N.N. Ledentsov, and D. Bimberg Appl. Phys. Lett. 74, 2815 (1999).
[6] K. Kuldova, V. Krapek, A. Hospodkova, J. Oswald, J. Pangrac, K. Melichar, E. Hulicius, M. Potemski, and J. Humlicek, Phys. Stat. Sol. (c) 3 (2006) 3811.
[7] A. Hospodkova, E. Hulicius, J. Oswald, J. Pangrac, T. Mates, K. Kuldova, K. Melichar, and T. Simecek, J. Cryst. Growth 298, (2007) 582-585
[8] K. Nishi, H. Saito, S. Sugou, and J. Lee, Appl. Phys. Lett. 74, 1111, (1999)
[9] D. Pan, E. Towe, and S. Kennerly, Appl. Phys. Lett. 73, 1937 (1998)
[10] M. Bayer, P. Hawrylak, K. Hinzer, S. Fafard, M. Korkusinski, Z. R. Wasilewski, O. Stern, and A. Forchel, Science 291, 451 (2001)
[11] W. Sheng, and J-P Leburton, Phys. Stat. sol. (b) No. 1, 394-404 (2003)
[12] P. W. Fry et *al*., Physica E 7 (2000) 408-412
[13] P. W. Fry et *al*., Phys. Rev. Lett. 84, 9007 (2000)
[14] P. Jin at *el*., Appl. Phys. Lett. 85, 2791 (2004)
[15] B. D. Geradot et *al.*, Appl. Phys. Lett. 90, 041101 (2007)
[16] M. M. Vogel et *al.*, Appl. Phys. Lett. 91, 051904 (2007)
[17] Quantum Semiconductor structures By C. Weisbuch and B. Vinter, By Claude Weisbuch, Borge Vinter Edition: 3, Published by Elsevier, 1991 ISBN 0127426809, 9780127426808.
[18] A. D. Andreev et *al.*, Appl. Phys. Lett. 87, 213106 (2005)
[19] Weidong Sheng et *al*., Appl. Phys. Lett. 80, 2755 (2002)
[20] Gerhard Klimeck *et al.*, "Atomistic Simulation of Realistically Sized Nanodevices Using NEMO 3-D: Part I - Models and Benchmarks", IEEE Trans. on Elect. Dev., Vol. 54, Pg: 2079 - 2089 (2007); *ibid* "Atomistic Simulation of Realistically Sized Nanodevices Using NEMO 3-D: Part II - Applications", Pg: 2090 - 2099 (2007)
[21] G. Klimeck et *al.*, Computer Modeling in Engineering and Science (CMES) Volume 3, No. 5 pp 601-642 (2002).
[22] P. Keating, Phys. Rev., Vol 145, no 2 pp. 637-644, May 1966
[23] Shu-Shen Li, and Jian-Bai Xia, J. of App. Phys. 88, 7171 (200)
[24] T. B. Boykin, G. Klimeck, R. C. Bowen, and F. Oyafuso, Phys. Rev. B 66, 125207 (2002); T.B. Boykin et al., Phys. Rev. B. 69, 115201, No 11 (2004); M. Luisier et al., Phys. Rev. B 74, 205323 (2006); T. B. Boykin et al., Phys. Rev. B 66, 125207 (2002); T. B. Boykin et al., Physical Review B, Vol 63, pg. 245314 (2001).
[25] G. Klimeck et *al*., Superlattices and Microstructures, Vol. 27, No. 2/3, Mar 2000, pp. 77-88
[26] R. C. Bowen et *al*., J. of Appl. Phys. 81, 3207 (1997).
[27] S. Lee et *al.*, Phys. Rev. B 66, 235307 (2002).
[28] R. Rahman et *al.*, Physical Review Letters, Vol 99, pg 036403 (2007).
[29] G.P. Lansbergen et *al.*, "Gate induced quantum confinement transition of a single dopant atom in a Si FinFET", Nature Physics, Vol. 4, pg. 656 (2008); Gabriel P.Lansbergen1 et *al.*, , IEEE IEDM, San Francisco, USA, Dec. 15-17, 2008.
[30] N. Kharche et *al.,* Applied Phys. Lett. Vol. 90, 092109 (2007)
[31] Muhammad Usman, Hoon Ryu, Insoo Woo, David Ebert, and Gerhard Klimeck, Accepted for publication in *IEEE* Trans. on Nanotechnology, to appear in 2009
[32] T. B. Boykin et *al*., Phys. Rev. B 65, 035202 (2001)
[33] A. D Andreev et *al*., Appl. Phys. Lett. 87, 213106 (2005)
[34] J. A. Barker et *al*., Phys. Rev. B 61, 13840 (2000)
[35] Seungwon Lee et *al*., Phys. Rev. B 63, 195318 (2001)
[36] G. Bester and A. Zunger, Phys. Rev. B 71, 045318 (2005)
[37] Shaikh Ahmed et *al*., accepted in Springer Encyclopedia for Complexity, 2008. Full paper at arXiv:0901.1890v1

Authorized licensed use limited to: Purdue University. Downloaded on October 19, 2009 at 15:42 from IEEE Xplore. Restrictions apply.